

Influence of Low and High Frequency Inputs on Spike Timing in Visual Cortical Neurons

Lionel G. Nowak, Maria V. Sanchez-Vives and David A. McCormick

Section of Neurobiology, Yale University School of Medicine, 333 Cedar Street, New Haven, CT 06510, USA

Cortical neurons *in vivo* respond to sensory stimuli with the generation of action potentials that can show a high degree of variability in both their number and timing with repeated presentations as well as, on occasion, a high degree of synchronization with other cortical neurons, including in the gamma frequency range of 30–70 Hz. Here we examined whether or not this variability may arise from the intrinsic mechanisms of action potential generation in cortical regular spiking, fast spiking and intrinsic burst-generating neurons maintained *in vitro*. For this purpose, we performed intracellular recordings in slices of ferret visual cortex and activated these cells with the intracellular injection of various current waveforms. Some of these waveforms were derived from barrages of postsynaptic potentials evoked by visual stimulation recorded *in vivo*; others were artificially created and contained various amounts of gamma range fluctuations; finally, others consisted of swept-sinewave current (ZAP current) functions. Using such stimuli, we found that, as expected given the resistive and capacitive properties of cortical neurons, low frequencies have a larger effect on the membrane potential of cortical neurons than do higher frequencies. However, increasing the amount of gamma range fluctuations in a stimulus leads to more precise timing of action potentials. This suggests that different frequencies play different roles, low frequencies being efficient for depolarizing cells with high frequencies increasing the precision of action potential timing. In parallel to increases in temporal precision, the addition of higher frequency components increases the range of interspike intervals present in the action potential discharge. These results suggest that higher frequency components such as gamma range fluctuations may facilitate the generation of action potentials with a high temporal precision while at the same time exhibiting a high degree of variability in interspike intervals on single trials. This temporal precision may facilitate the use of temporal codes or the generation of precise synchronization for the transmission and analysis of information within cortical networks.

Introduction

How do visual cortical neurons encode information in their action potential trains? The answer to this fundamental question is critical to our understanding of the organization of cortical networks and the mechanisms by which they operate (e.g. see Shadlen and Newsome, 1994), but, surprisingly, it is a question for which we still have no clear answer, despite decades of investigation. One reason for this state of affairs is the variability of neuronal responses in the cerebral cortex. As a result of this variability of single cortical neuron responses, two broad theories of action potential encoding have arisen. One theory holds that only the average rate of action potential generation in any given neuron is important (so-called 'rate code'), with significant events or details being encoded by the average activity of a pool of neurons (reviewed by Shadlen and Newsome, 1994; Rieke *et al.*, 1997). Another view, known as the 'pulse' or 'temporal' code, is that the timing of action potentials,

and in particular the temporal relationship of action potential generation between neurons, is information rich (e.g. see Softky, 1995; Rieke *et al.*, 1997).

In general, extracellular recordings from cortical neurons in anesthetized (Shiller *et al.*, 1976; Rose, 1979; Dean, 1981; Tolhurst *et al.*, 1983; Bradley *et al.*, 1987; Scobey and Gabor, 1989; Swindale and Mitchell, 1994) and awake behaving (Vogels *et al.*, 1989; Snowden *et al.*, 1992; Softky and Koch, 1993) animals have revealed a large variability in both the number of action potentials and the timing of these action potentials in response to repeated presentation of a constant sensory stimulus. Two exceptions to this, which to some degree are related, are the presence of bursts of action potentials and rhythmic oscillations (see below). In anesthetized animals, this variability arises at least in part from the disruptive influence of spontaneous intracortical and thalamocortical rhythms (e.g. Arieli *et al.*, 1996), while the variability in the number of action potentials generated per stimulus in the primary visual cortex of awake and behaving animals results in part from small eye movements (Gur *et al.*, 1997). Controlling for the effects of anesthesia by working with awake and attentive animals and controlling for small eye movements results in a significant reduction in response variability, although these manipulations by no means abolish it (Gur *et al.*, 1997).

Does the remaining variability reflect that found in the presynaptic inputs to the recorded cell, or does each neuron along the path of activity add variance through intrinsic mechanisms? Response variability, both in timing and in amplitude, is not a novel feature of cortical neurons and is present in both the discharges of retinal ganglion cells and the thalamocortical neurons of the dorsal lateral geniculate nucleus (Troy and Lennie, 1987; Croner *et al.*, 1993; Hartveit and Heggelund, 1994), although the amplitude of this variance depends critically upon the dynamic features of the stimulus used (e.g. see Berry *et al.*, 1997). Recent *in vitro* investigations by Mainen and Sejnowski (1995) indicate that regular spiking neurons of the cerebral cortex are capable of remarkably precise action potential timing and that this precision depends upon the presence of higher frequencies in the membrane fluctuations associated with synaptic activation (see also Tang *et al.*, 1997). These results suggest that the variability in spike timing and intensity *in vivo* are a reflection of variations in the underlying synaptic barrages from one stimulus presentation to the next.

In contrast to response variability of cortical responses, other investigations have revealed 'replicating patterns' of action potentials (also called 'favored patterns' or 'spatiotemporal firing patterns'), i.e. sequences of action potentials emitted with constant intervals, that are repeated above what would be expected by chance. Such patterns have been identified in visual cortex (Dayhoff and Gerstein, 1983; Lestienne and Strehler, 1987; Villa and Fuster, 1992; Bair and Koch, 1996), in auditory

thalamus and cortex (Abeles and Gerstein, 1988; Villa and Abeles, 1990) and in the frontal cortex of awake behaving monkeys (Abeles *et al.*, 1993).

An additional example of precision in action potential generation is also found in the generation of synchronized activity in the gamma frequency range (30–70 Hz) in the visual cortex. The generation of this pattern of activity is often associated with the occurrence of repetitive burst discharges (Gray *et al.*, 1990), which appear to be characteristic of an electrophysiologically distinct subgroup of cortical pyramidal cell (Gray and McCormick, 1996), and may be associated with significant synchronization with other cortical neurons, depending upon configuration of the stimulus (Engel *et al.*, 1991).

Are these three characteristics of cortical processing (variability, precision and higher frequency fluctuations) related in any fashion? Here we examined the consequences of higher frequency activity, in particular gamma range fluctuations, on the precision of spike timing as well as its variability. For that purpose, we used current waveforms containing variable amounts of gamma range fluctuations that were injected into intracellularly recorded neurons in slices of ferret visual cortex. Some of the stimuli used were derived from real visual responses. Others were artificial stimuli for which the proportion of gamma range fluctuations could be precisely varied. The results we obtained show that increasing the amount of gamma range fluctuations in the stimulation leads to both: (i) an increase in the precision of spike timing; and (ii) an increase in interspike interval variability on single trials.

Materials and Methods

Preparation of the Slices

Male or female ferrets were deeply anesthetized with sodium pentobarbital (35 mg/ml, i.p.) and killed by decapitation. A block of cortex containing the primary visual cortex was removed and placed in cold (5°C) artificial cerebrospinal fluid in preparation for sectioning. The artificial cerebrospinal fluid was oxygenated with 95% O₂, 5% CO₂ to a final pH of 7.4 and contained (in mM): NaCl 126, KCl 2.5, MgSO₄ 1.2, Na₂HPO₄ 1.25, CaCl₂ 1.2, NaHCO₃ 26, dextrose 10. Sections 400 μm thick were cut on a Vibratome (Lancer Corporation) and placed in an interface-style recording chamber (Fine Science Tools) and allowed to recover for at least 1 h before recording. The slice chamber temperature was kept at 35.5 ± 0.5°C.

Intracellular recording was performed with microelectrodes formed from beveled microelectrodes pulled from 1B100F micropipette glass (World Precision Instruments) on a Sutter Instruments P-80/PC micropipette puller, filled with 4 M potassium acetate, and had a final resistance ranging from 60 to 80 MΩ.

Recording

All neurons were recorded in layer II/III. Only those cells that maintained a stable resting membrane potential and responded to depolarizing current injection with the generation of trains of action potentials were included for analysis. Cells were grouped into one of three classes, according to established criteria (McCormick *et al.*, 1985): regular spiking, intrinsic bursting and fast spiking.

Stimuli

In addition to the conventional square current pulses, several different types of stimuli were injected into intracellularly recorded neurons through the use of the Clampex 6.0 software program (Axon Instruments). One pattern of stimuli consisted of a swept sinusoidal current (ZAP current; cf. Hutcheon *et al.*, 1996) that was obtained by digitally capturing the output of a signal generator. Two such stimuli consisted of either a function that varied in frequency from 2 to 20 Hz over ~3 s to one that varied from 10 to 200 Hz and are referred to as

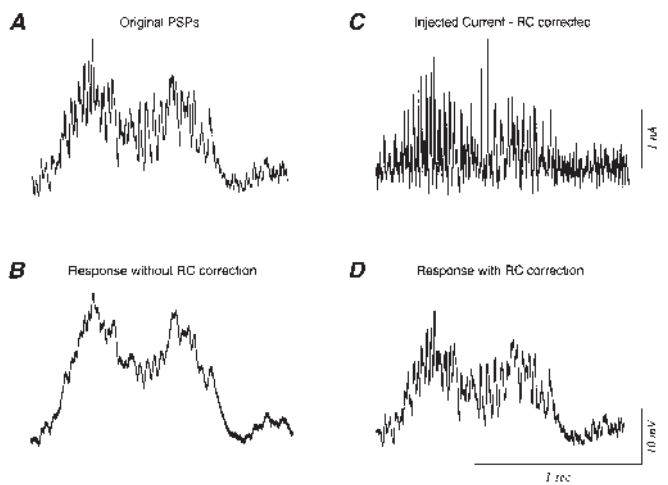


Figure 1. Method for calculation of injected current waveform to mimic postsynaptic potentials. (A) Barrage of synaptic potentials in a cortical neuron (chattering cell) during the movement of a bar across its receptive field. The cell was intracellularly recorded in cat's area 17. The membrane potential was maintained hyperpolarized by constant current injection to prevent firing of action potentials. (B) Response of a RC circuit ($R_{in} = 50 \text{ M}\Omega$, $C_{in} = 0.47 \text{ nF}$, $\tau = 23.5 \text{ ms}$) to the injection of the synaptic potential waveform shown in A. The RC characteristics led to the filtering of the PSP sequence. While the low frequencies are well preserved, the amplitude of the high frequency components are decreased in amplitude. These RC characteristics can be compensated for using the calculation described in the Materials and Methods. Compensation for the RC properties of this model circuit yields the waveform in C ('injected current'). (D) When this current was injected into the RC circuit, the resulting membrane deviation is identical to that of the original PSP sequence (compare D with A). Scale bars in D also apply to A and B.

'Sine20' and 'Sine200' (Figures 11 and 12). The peak-to-peak amplitude of these sine wave functions was adjusted to be 1 nA.

A second type of current waveform was constructed from visually evoked responses. Barrages of postsynaptic potentials (PSPs) were intracellularly recorded *in vivo* in response to an optimal visual stimulus (moving bar) in a layer II/III chattering pyramidal cell in cat area 17 while the cell was maintained hyperpolarized to prevent action potential generation (cf. Gray and McCormick, 1996 for details of the preparation). In this particular chattering cell, the synaptic barrages exhibited a significant amount of fluctuation in the 20–70 Hz frequency range, as has been observed previously (Jagadeesh *et al.*, 1992). Three of the visually evoked synaptic barrages were used for this study (hereafter referred to as 'PSP 9', 'PSP 10' and 'PSP 16', the number referring to the trial number in the original cell). These three synaptic responses were selected for their different amounts of gamma range fluctuations (Figure 5). One of these PSP sequences is shown in Figure 1A ('original PSP').

We sought to examine the response of cortical neurons *in vitro* to the injection of these PSP sequences through an intracellular microelectrode. However, merely injecting the PSP waveform into a cell maintained *in vitro* would result in a low-pass filtered version of the original PSP sequence, owing to the resistive and capacitive properties of the original cell as well as those of the injected cell (e.g. Fig. 1B). Therefore, we compensated for the parallel resistive and capacitive (RC) characteristics of the membrane of the original chattering cell according to the following formula:

$$I_{\text{inject}} = I_{\text{Res}} + I_{\text{Cap}} = V/R_{in} + (dV/dt)C_{in} \quad (1)$$

The values of R_{in} and C_{in} for the chattering cell from which the PSPs were recorded were estimated to be 35 MΩ and 429 pF, based upon the response of the cell to repetitive 0.2 nA hyperpolarizing current pulses at rest. Owing to the use of differentiation to obtain I_{Cap} , it was necessary to apply a boxcar-style filter with 11 adjacent data point averaging to smooth the resulting function using Clampfit 6.0. The resulting function (Fig. 1C) was injected into intracellularly recorded neurons *in vitro*, without additional compensation for the RC-characteristics of the recorded cells,

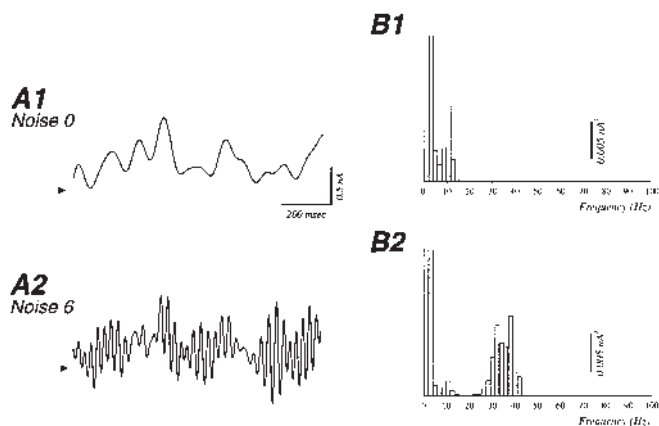


Figure 2. Shape and power spectrum of two of the current waveforms used for injection. In *A1* and *A2* are displayed two artificially created current waveforms named Noise 0 and Noise 6. The trace in *A1* consisted of low frequencies only, as revealed by the power spectrum presented in *B1*. A pattern made of high frequency (30–40 Hz) fluctuation has been added to this waveform to produce the current waveform shown in *A2*. The addition of the high frequency pattern resulted in a shift in the power spectrum to higher frequencies (power spectrum in *B2*). Arrows on the left of current traces in *A1* and *A2* indicate 0 nA. Bins for frequencies <4 Hz are truncated.

since this is one variable determining the postsynaptic response of these neurons (Fig. 1*D*).

A third series of current waveforms corresponds to artificial stimuli, hereafter referred as to ‘noise’ stimuli, that were created from a series of random numbers that were digitally filtered in order to emphasize their low or high frequency content. The results obtained with two (out of eight) such stimuli are presented in this study. The first one corresponds to a low frequency pattern (Fig. 2*A1*). Figure 2*B1* illustrates the corresponding power spectrum, which shows a peak at 10 Hz. To this pattern was added an additional component containing frequencies between 30 and 40 Hz, and this waveform is referred to as ‘Noise 6’ (Fig. 2*A2*). The net current added by the 30–40 Hz pattern was zero, since the negative phases canceled the positive phases. In other words the two stimuli are identical in terms of total current injected. The addition of the gamma frequency pattern, however, resulted in a shift of the power spectrum to higher frequencies (between 30 and 40 Hz, Fig. 2*B2*). The durations of the ‘PSP’ and ‘noise’ stimuli were 1–1.2 s. Each stimulus waveform was applied from 10 to 16 times with an intertrial interval of ~10–30 s to allow the cell to recover from the previous trial.

Measurements of Spike Timing Precision and Reliability

For analysis of spike timing and variability, data were acquired through a Cambridge Electronic Design digitizing system (CED 1401 plus). Action potentials were detected using a window discriminator and stored as time events with a precision of 10 μ s. Data analysis was performed with Spike2 software (CED) with custom designed program routines.

The analysis of the reproducibility of the spike timing was similar to that of Mainen and Sejnowski (1995), with some differences, and is illustrated for a regular spiking neuron in Figure 3. In Figure 3 are shown the response of a cell to the application of Noise 0 (Fig. 3*A*) and Noise 6 (Fig. 3*B*) stimuli. The same waveform current has been applied 16 times. For clarity, only a fraction of the response is displayed (0.1–0.25 s). The first step for the analysis consisted in constructing a peristimulus histogram with a bin width of 1 ms (Fig. 3*C* for Noise 0, Fig. 3*D* for Noise 6). The bin height was normalized by the number of stimuli, such that the height is 1 if the cell fired an action potential at the same time for all the stimulus presentations.

The next step consisted of defining an ‘event’, i.e. an action potential obtained with a sufficiently high temporal precision to yield large bin(s) in the peristimulus time histogram. To define an event, we arbitrarily chose a threshold value corresponding to a height of 0.2 (dotted line in histograms). An ‘event’ corresponds to the bin(s) larger than the threshold, plus the bin immediately adjacent to these, even if their height is lower than the threshold. This was necessary due to binning artifact.

For example, an action potential might have occurred at time 101.1 ± 0.1 ms on all trials except for one, where the latency may have been 100.9. Although this value is very similar to the others, it corresponds to another bin in the histogram. One event is delimited by the dashed lines and arrow in Figure 3*C* and another one in Figure 3*D*.

The variable *reliability* is a measure of the probability of observing an action potential at constant (within the limits of an event) latencies. It is defined as the cumulative sum of the bins that are larger than the threshold, divided by the cumulative sum for all the bins (or, in other words, the ratio of the number of spikes falling in bins >0.2 divided by the total number of spikes). A value of 1 would be obtained if the stimuli led to the firing of the cell with all spikes elicited at the same latencies. Notice that the calculation of reliability excludes those bins that are lower than the threshold, even if they participate in an event.

The *precision* variable gives a measure of the temporal jitter of spike latency. First the standard deviation (SD) of the latency of the spike corresponding to each event is calculated. Then the SD for all the events is averaged. The precision measure, referred to as *jitter*, corresponds to this average SD and therefore, increases in jitter (i.e. increased SD) are associated with decreases in the precision of action potential timing.

For bursting neurons ($n = 2$; bursting neurons being defined as those neurons that present a bimodal interspike intervals distribution in response to current pulse injections), the analysis has been restricted to the first spike of the bursts. For two other cells, the firing rate for some period of the stimuli was too high to allow an unambiguous delimitation for some events. This ambiguity was solved by removing the spikes falling <3 ms after the preceding ones, and restricting the analysis to the remaining spikes.

Measurements of Interspike Interval Variability

For the measurement of interspike interval variability, we used the method designed by Holt *et al.* (1996). The interspike interval (Δt_i) is the latency difference of two successive action potentials in a spike train:

$$\Delta t_i = t_i - t_{i-1}$$

where t_i is the latency for the i th action potential elicited by the stimulus.

The classical measure of interspike variability is the variation coefficient (C_v), which corresponds to the standard deviation of the interspike intervals divided by the mean interspike interval. However, this measure cannot be applied to spike trains with variable rate over time (for further discussion see Softky and Koch, 1993; Holt *et al.*, 1996). Another measure of variability, which is not influenced by the rate variation, is the C_{v2} measure proposed by Holt *et al.* (1996):

$$C_{v2} = 2|\Delta t_{i+1} - \Delta t_i| / (\Delta t_{i+1} + \Delta t_i)$$

This measure of variability compares only two adjacent interspike intervals. For a cell firing Poisson-distributed action potentials, the C_{v2} is distributed uniformly between 0 and 2, with a mean close to 1. The C_{v2} has been calculated for all repetitions of a given stimulus. For bursting neurons the variation coefficient has been calculated only for the first spike of the bursts.

The stimulus protocols used here, as well as additional information, are available from <http://info.med.yale.edu/neurobio/mccormick/mccormick.html>.

Results

Eleven neurons were recorded in layer II/III of the ferret primary visual cortex for sufficient periods of time and stability to inject many or all of the various stimuli outlined in Materials and Methods and shown in Figures 2, 5 and 11. Of these 11 neurons, seven were classified as regular spiking neurons, two as burst-generating cells, and the remaining two as fast spiking neurons, following the criteria of McCormick *et al.* (1985). No chattering cells (Gray and McCormick, 1996) were recorded in this small sample of cells.

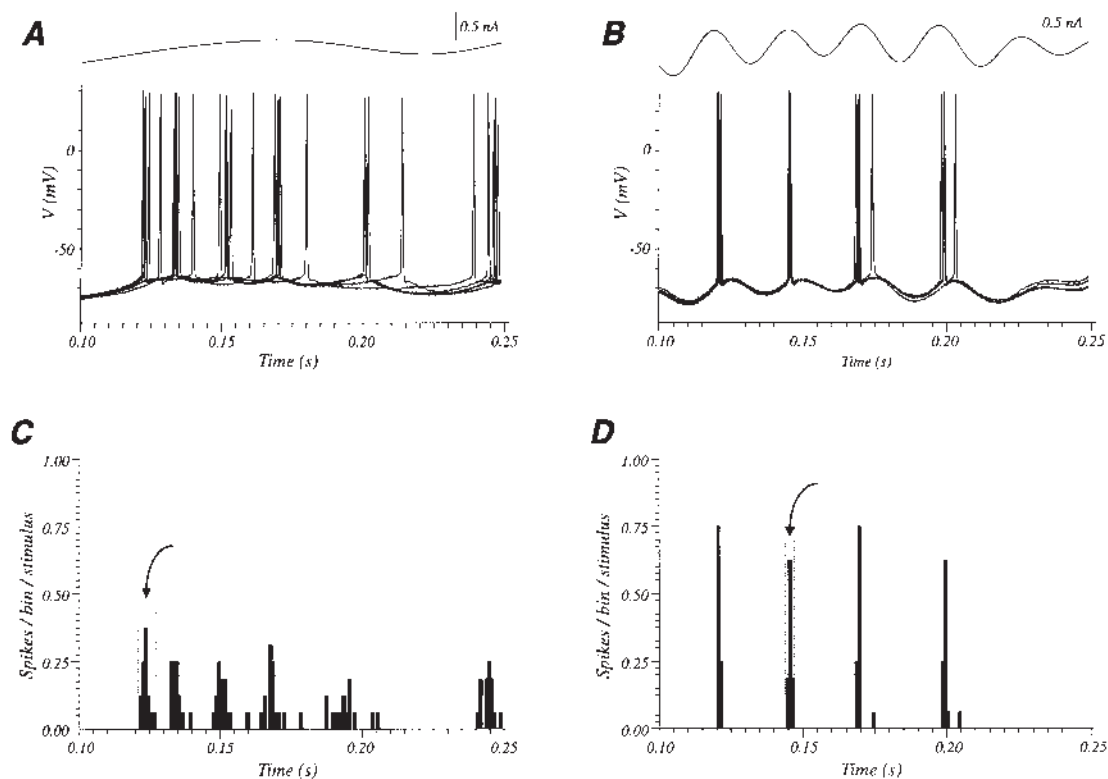


Figure 3. Measurements of spike timing jitter and reliability. The responses illustrated in *A* and *B* are eight (out of 16) superimposed responses to stimulation with Noise 0 (*A*) and Noise 6 (*B*) current waveforms (shown above voltage traces) in a regular spiking cell. Only a short portion of the original traces are shown. (*B*) PSTH constructed from the response of the cell to the same stimuli (Noise 0 in *C*, Noise 6 in *D*). Calculation of reliability and jitter of spike timing are based on such PSTHs. The dashed line and arrow in *C* delineate an 'event'. More details in text.

Comparison of Current Pulses and 'PSP' Sequences in the Three Cell Types and Transmission of Gamma Range Fluctuations

Compared to the *in vivo* situation, the main advantage of the *in vitro* preparation is the very low background synaptic activity. This virtually suppresses one of the parameters that could be a considerable source of timing variability. The other advantage of the protocol we used is that the same 'visual drive' could be mimicked in different cell types, although we cannot pretend that the current injection completely reproduced the visual activation (e.g. the changes in conductance and the distribution of these conductances related to synaptic responses are not reproduced by the current waveforms).

Figure 4 illustrates examples of the responses for the three cell types to the injection of constant current pulses as well as a current waveform (PSP 16) derived from a barrage of PSPs recorded in a chattering cell *in vivo* in response to the presentation of a moving bar visual stimulus (see Figure 1 and Materials and Methods). Regular spiking neurons responded to the injection of a constant current pulse with a train of action potentials that exhibited some spike frequency adaptation (Fig. 4*A*) and to the injection of PSP 16 with the generation of single and clusters of action potentials that varied according to the stimulus (Fig. 4*D*). Fast spiking neurons responded to constant current pulses with the generation of high frequency (up to 500 Hz) trains of relatively short duration (0.5 ms at half amplitude) action potentials that exhibited little spike frequency adaptation (Fig. 4*B*). Like regular spiking cells, fast spiking neurons also responded to the injection of PSP 16 with the generation of single or clusters of action potentials (Fig. 4*E*). Intrinsic burst-

generating neurons responded to the intracellular injection of a constant current pulse with the generation of bursts of action potentials. Typically the first burst contained a larger number of action potentials than those that followed; eventually the bursts were followed by a train of single action potentials (Fig. 4*C*). Injection of PSP 16 into intrinsic burst-generating cells generated a mixture of single spikes and spike bursts (Fig. 4*F*, see also Fig. 10). These data suggest that all three cell types respond quite well and in a somewhat similar manner to a complex stimulus such as that represented by PSP 16.

Indeed, as illustrated in Figure 5, analysis of the power spectrum of the frequencies represented in the spike output of these three different cell types revealed that all three exhibited significant modulation in the frequency components present in the injected waveform, including in the so-called gamma frequency range (30–70 Hz). At the top of Figure 5 are presented the power spectra obtained by fast Fourier transform of the three current waveforms derived from visually evoked synaptic responses. These current waveforms displayed different amounts of power for different frequencies: the stimulus 'PSP 9' contains a peak centered at 30 Hz and an additional peak at 60 Hz (Fig. 5*A1*); 'PSP 10' a peak centered on 40 Hz (Fig. 5*A2*); 'PSP 16' exhibited three peaks at 30, 40 and 50 Hz (Fig. 5*A3*). The power spectra calculated for the membrane potential of the cells (not illustrated) were very similar to that of the current injected. However, the membrane response of the cells exhibited a greater decrease of power for higher frequencies in comparison to the lower frequencies, a consequence of the resistive and capacitive characteristics of the cortical neurons.

To determine if the gamma range fluctuations were

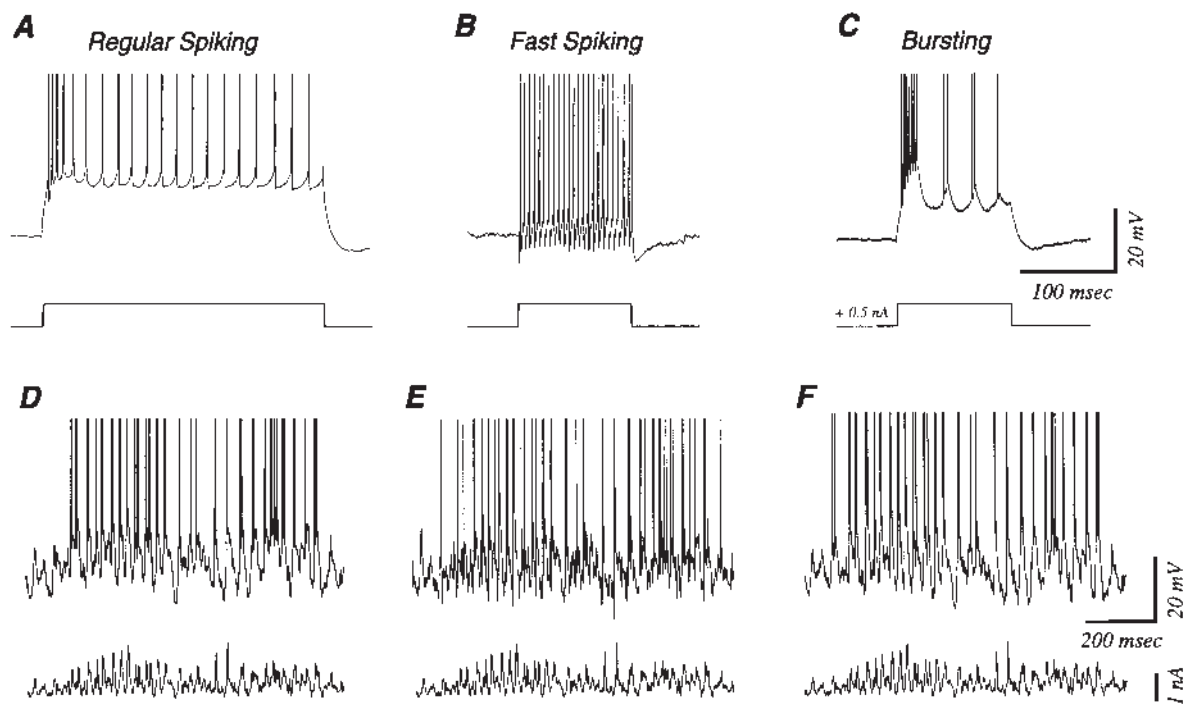


Figure 4. Responses of different cell types to constant current pulses and to a current waveform derived from a visual response. The response of a regular spiking cell is shown for current pulses in *A* and for the current waveform PSP 16 in *D*. The response of a fast spiking cell is shown for current pulses in *B* and for the current waveform PSP 16 in *E*. The response of a bursting neuron is shown for current pulses in *C* and for the current waveform PSP 16 in *F*. The response in all three cells are from the injection of a 0.5 nA current pulse. The responses to both the current and injected waveform are single trials. Scale bars in *C* apply to *A* and *B*. Scale bars in *F* apply to *D* and *E*. Action potentials are truncated.

effectively transmitted to the output of the neurons, we performed power spectrum analysis of the spike trains induced by the intracellular injection of these currents. For this purpose, the spike train was converted into a waveform channel, by replacing each action potential by a waveform fragment (a raised cosine bell, the full width of the bell at the bottom being 2 ms). The waveform channel derived from the spike train could then be subjected to a power spectrum analysis (the duration of the waveform fragment was sufficiently short to prevent alteration of the power spectrum at the frequencies shown). The results of such analyses are shown in row *B* of Figure 5 for a regular spiking neuron, in row *C* for a bursting neuron and in row *D* for a fast spiking neuron (same cells as Fig. 4). Comparing the power spectrum along one column, it is clear that the features in the injected current appear in the spike output of each of the different cell types. The power spectra in *B1*, *C1* and *D1* show a broad peak, evenly split in two, centered, like that for the current, on 30 Hz. Similarly the peak centered on 60 Hz in Figure 5*A1* is also found for the three cells (Fig/ 5*B1*, *C1* and *D1*). These results indicate that the spike output of regular spiking, fast spiking and intrinsic bursting neurons is to a fair degree a faithful representation of the injected waveform.

To examine this hypothesis quantitatively, we calculated the correlation coefficient for the bin height present in the power spectra of the current versus that contained in the spike response. We restricted this analysis to the bins between 10 and 80 Hz (above 80 Hz the power spectra for the currents were essentially flat, while below 10 Hz the very high bins for low frequencies and DC component would have led to artificially strong correlations). The correlation coefficients (r) obtained for the three cells and stimuli of Figure 1 were between 0.71 and 0.89 for PSP 9, 0.55 and 0.77 for PSP 10, and 0.71 in all the cases

for PSP 16 (all correlations were statistically significant). These results suggest that the temporal organization of the synaptic current input is replicated in the output.

However, the correlation coefficients indicate that only ~50% (r^2) of the output power spectrum of a cell can be traced back to its input. This indicates that there are additional sources of noise. One obvious source of noise might be the small number of spikes. Another could arise from the conversion of the transmembrane current to the spike discharge. A third one is related to the membrane properties (RC characteristics, accommodation and burstiness among others) of the neurons. If the membrane properties were responsible, then we would expect that part of temporal features of the discharge of one cell be preserved from one stimulus type to another. This would lead to a significant correlation, for the *same* cell, between the power spectrum of the spike discharge to *different* stimuli. A significant correlation was observed in only one out of six cases. (For the three cells shown in Figure 5, the correlations between PSP 16 versus PSP 10 were not tested because the power spectra of the current themselves showed a significant, although poor, correlation.) The significant case showed a correlation coefficient of 0.32 only. Therefore, as far as frequencies between 10 and 80 Hz are concerned, the temporal pattern in the output of a cell is likely to be much more strongly determined by its synaptic drive than by its membrane properties.

Influence of Higher Frequencies on Precision and Reliability of Spike Generation

Having shown that gamma range fluctuations are transmitted from the input to the spike output, we can examine in more detail the temporal organization of the spike train. The first aspects we studied were the *reliability* and *jitter* (precision) of

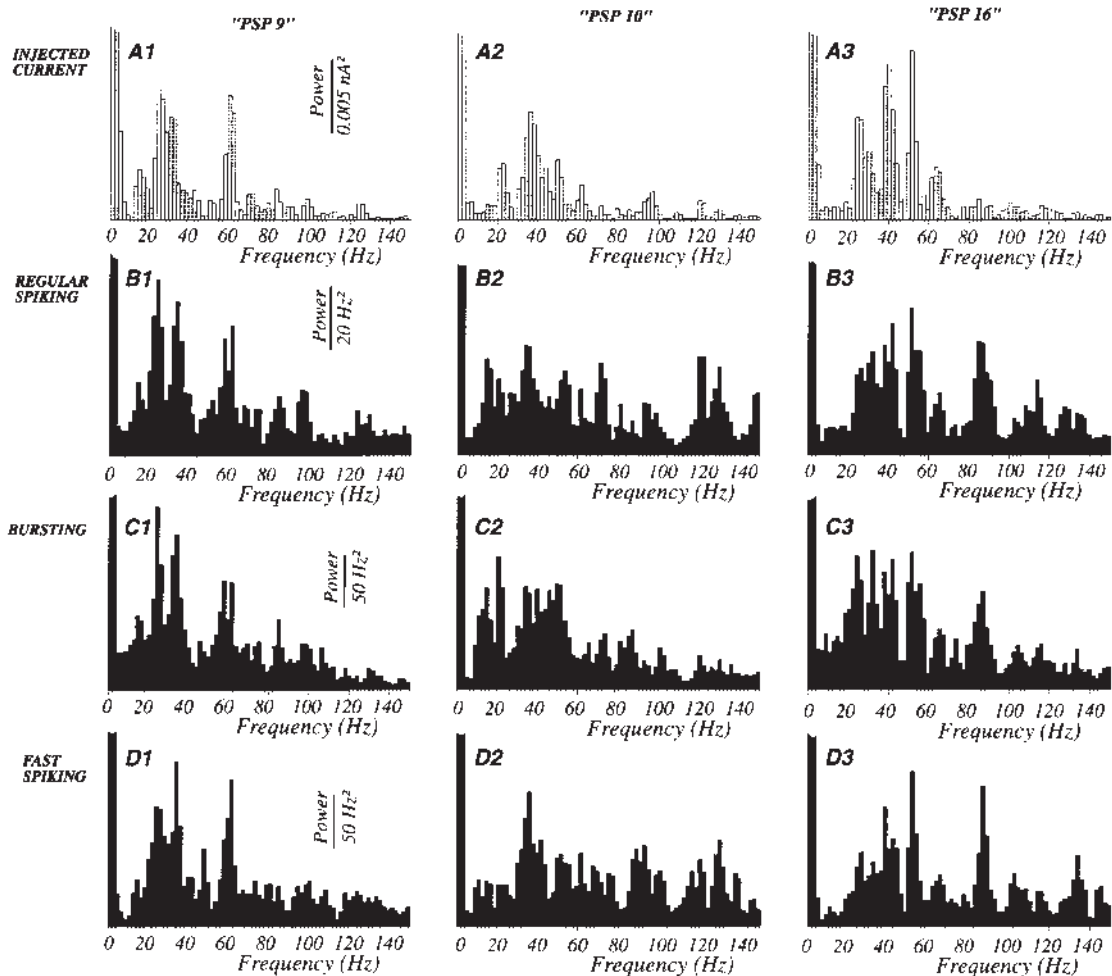


Figure 5. Transmission of gamma range fluctuation from the injected current to spike output. (A1–3) Histograms illustrating the power spectrum of the current waveform derived from three different synaptic responses obtained in response to visual stimulation *in vivo* (labeled ‘PSP 9’, ‘PSP 10’ and ‘PSP 16’ at the top of the figure). (B1–3) Power spectrum analysis of the spike response of a regular spiking cell to the current waveforms. The spike train, consisting of discrete events, have first been converted to a continuous waveform, before analysis of its power spectrum by fast Fourier transform. (C1–3) The same analysis for a bursting neuron. (D1–3) The same analysis for a fast spiking cell. Interestingly, an additional peak at 90 Hz was observed consistently in all the cells activated by PSP 16, although this peak was not obvious in the stimulus. Scale in histograms in column 1 apply to the two other columns. The bins for frequencies <4 Hz are truncated.

firing (see Materials and Methods), that is to say: does a cell always fire at the same time when subjected to the repeated presentation of the same stimulus? Figure 6 illustrates the timing of action potentials in a regular spiking neuron. The response to the repeated injection of a constant current pulse is shown in Figure 6A. Although the same current intensity was used, the raster plot indicates that the latency for action potentials was quite variable from one trial to the next, especially for the action potentials that occurred late in the spike train.

In contrast, after the injection of a current waveform that contains a large amount of gamma range fluctuation (PSP 16, Fig. 6B), action potentials appeared to be elicited with very similar latencies from one trial to the next, as indicated by the alignment of dots in the raster plot. The maintenance of a constant latency is visible for both the spikes that occurred early and those that occurred late in the discharge. To quantify the reproducibility of spike timing, we use the measures of *jitter* and *reliability* introduced by Mainen and Sejnowski (1995) (see Materials and Methods). In that case the *reliability* increased from 0.249 with the constant current pulse to 0.932 with PSP 16. The *jitter* of spike timing decreased from 0.98 with current pulses to 0.175

ms with PSP 16. This means that, with PSP 16, the probability that action potentials occurred at the same latency increased. In addition, the temporal jitter for that latency decreased with PSP 16.

Artificial stimuli were used in order to determine what frequencies are more likely to increase the precision of spike timing. One stimulus contained only low frequencies (Noise 0, e.g. Fig. 2). When injected into a cell, this stimulus resulted in an improvement in the precision of spike timing in comparison to constant current injection (Fig. 6C; compare with 6A), yet the precision was still less than that obtained with the injection of PSP 16. Figure 6D shows results obtained with the injection of an artificial current waveform that contained mostly high frequencies between 30 and 40 Hz (Noise 6, power spectrum in Fig. 2). In comparison to Noise 0, the presence of these gamma-frequency oscillations significantly increased the reliability and decreased the jitter of spike timing. With the pattern dominated by low frequencies (Noise 0) the reliability was 0.537 and the jitter was 1.13. With the pattern dominated by high frequencies (Noise 6), the reliability increased to 0.758 and the jitter decreased to 0.57 ms.

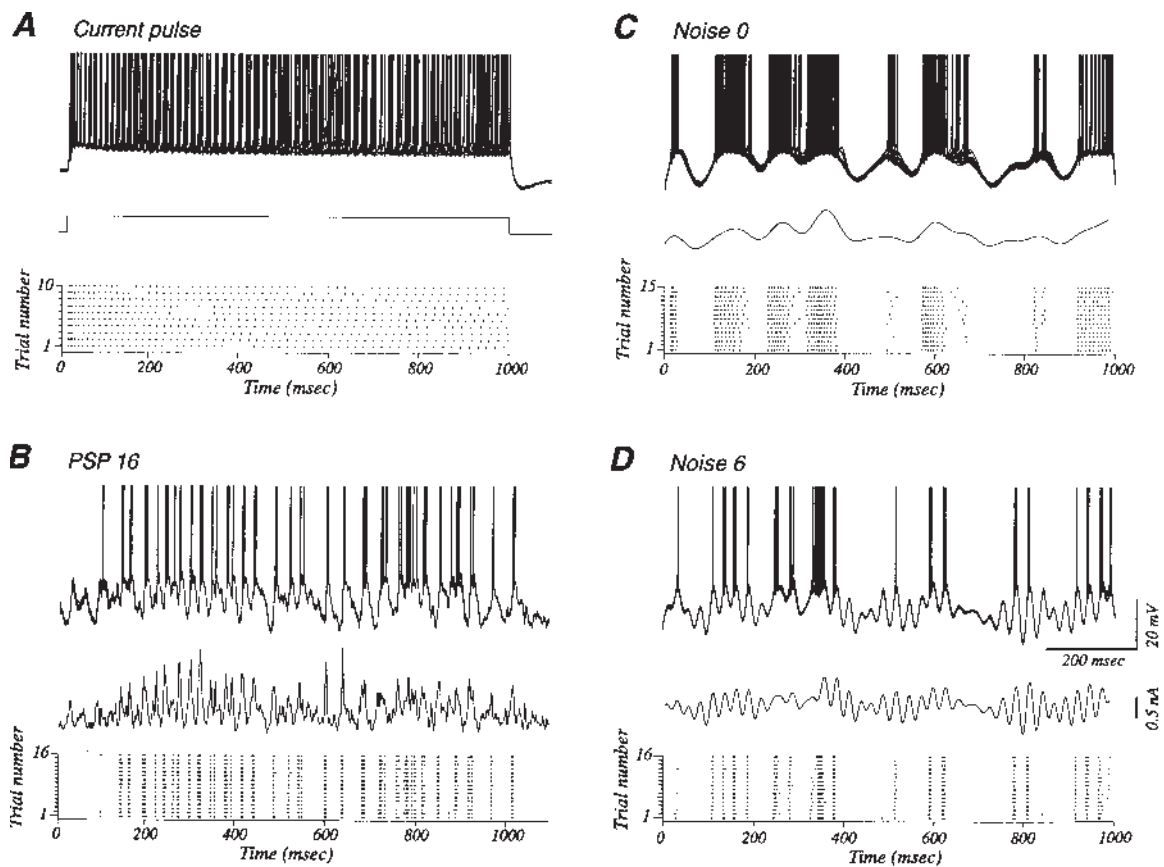


Figure 6. Reliability and jitter of spike timing in a regular spiking cell. (A) Upper: response of the cell to the application of 10 current pulses of same intensity. Below is shown a raster plot illustrating the variability of spike latency from one trial to the next. (B) Response of the cell to a current waveform derived from a visually evoked response. Ten of the 16 traces obtained are shown superimposed in the upper part. The alignment of the dots in the raster plot indicates improvement in the precision of spike timing. (C) Response of the cell to an artificial current waveform dominated by low frequency components. Ten of 15 traces shown superimposed in the upper part. (D) Response of the cell to an artificial current waveform dominated by high frequency components. Ten of the 16 traces are superimposed in the upper part. The lower part is a raster plot of the spike response. Scale bars in D apply to A–C. Action potentials are truncated.

Influence of Increased Variability of Injected Current on Variability of Spike Generation

The previous results demonstrated that increasing the amount of higher frequency (>10 Hz) components in the injected waveform increased the temporal precision with which action potentials were produced with repeated presentations of the same stimulus. However, increasing the range of frequencies present in the injected current also results in a larger range of frequencies represented in the spike discharge on any given trial, and therefore an increase in the variation between interspike intervals *within* single trials. Note that the above results on timing precision were related to the latency of *one* action potential *from one stimulus to the next*. What is examined now are the interspike intervals, i.e. the amount of time separating *two* action potentials *in the same spike train*. The variability of interspike intervals is illustrated in Figure 7 for the same cell as in Figure 6. The variation coefficient of the interspike intervals (C_{V2}) has been determined using the method of Holt *et al.* (1996) (see Materials and Methods).

The injection of constant current pulses results in trains of action potentials in which adjacent interspike intervals are similar in duration with relatively smooth variations in time (e.g. spike frequency adaptation; Fig. 6A). Quantification of the variability of these interspike intervals illustrates this low variability, and thus the regularity of action potential discharge. This is illustrated in Figure 7A, where the scattergrams presents the C_{V2}

values as a function of the mean value for the same two adjacent interspike intervals. The concentration of dots in the lower left corner indicates that successive interspike have similar durations. The histogram on the right of the scattergram represents the distribution of C_{V2} values, and these are low on average. In contrast to the results with a constant current pulse, the variation in interspike intervals is high in response to injection of PSP 16 (Fig. 7B), indicating that the duration of successive interspike intervals in this response could vary from very short to long (e.g. see Fig. 6B), reflected by large values of C_{V2} .

We next determined how the interspike variability evolves as a function of the amount of gamma range frequencies contained in the stimulus. With the artificial waveform that contained only a ~10 Hz frequency modulation of current (Noise 0) the variability of interspike intervals within a trial remained low (Fig. 7C; note histogram). When gamma range fluctuations were added to the same stimulus (Noise 6) a considerable increase in variability of interspike intervals within the response was obtained, owing to the increased range of frequencies represented in the injected current (Fig. 7D; note histogram).

Relationship between Reliability, Jitter and Variability

Summarizing the results on between-trial reliability and jitter (precision), and within-trial variability in response to the injection of current pulses (current pulse stimuli; $n = 6$ cells), artificial stimuli with and without gamma range fluctuations

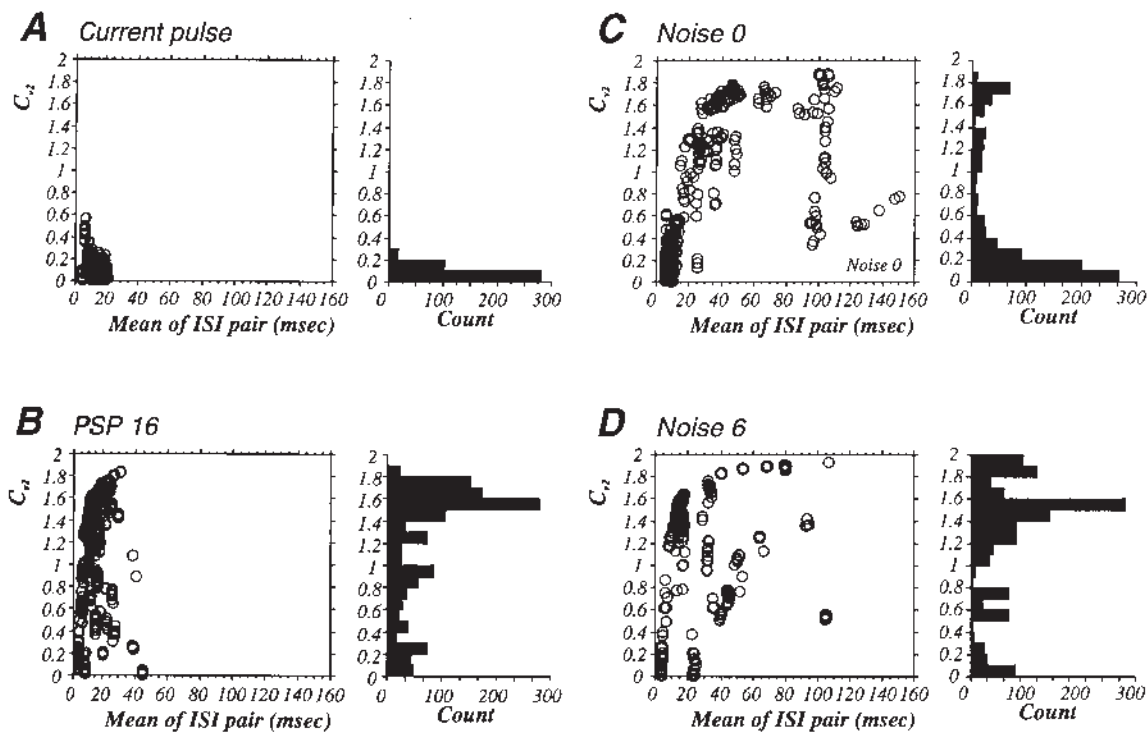


Figure 7. Variability of interspike intervals. Same cell as in Figure 6. For each stimulus are presented a scatter plot of C_{v2} (the variation coefficient calculated from two adjacent interspike intervals) as a function of the mean value for these two interspike intervals. On the right of each scatter plot is shown a histogram of the distribution of C_{v2} values (bin width 0.1). Scatter plot and histograms in A–D correspond to current pulses, PSP 16, Noise 0 and Noise 6 stimuli respectively. The presence of several superimposed dots, especially in D, is the result of the similarity of spike latency, hence interspike intervals, from one trial to the next.

(Noise 0 and Noise 6; $n = 8$ cells), and in response to the injection of the ‘visual’ stimuli (PSP 16; $n = 11$ cells) demonstrate the relationship between these measures (presented in Figure 8 and Table 1). The injection of other visually evoked PSP sequences (PSP 10 and PSP 9) yielded results similar to those obtained with PSP 16, and therefore only the results obtained with this stimulus are presented.

As shown in Figure 8A1, the *reliability* increased when the amount of gamma range fluctuation present in the stimuli was higher. The reliability was significantly larger with PSP 16 compared to Noise 6 ($P = 0.0002$, unpaired *t*-test), and this was itself significantly larger than that obtained with Noise 0 ($P = 0.03$), which was larger than that obtained with current pulses ($P = 0.0007$).

In addition to an increase in reliability, an increase in the amount of gamma range fluctuation resulted in a decrease in spike timing jitter, as illustrated in Figure 8A2. There was no difference between current pulses and Noise 0 stimuli ($P = 0.2$). The jitter was lower for Noise 6 ($P = 0.005$ when compared with Noise 0), and still lower with PSP 16 ($P = 0.02$ when compared with Noise 6). Jitter and reliability are significantly correlated, as illustrated in Figure 8B1 ($\rho = -0.884$, $P < 0.0001$; Spearman rank correlation).

Changes in variability of interspike intervals within trials are summarized in Figure 8A3. Calculations are based on the mean C_{v2} value for each stimulus condition. Increasing the amount of gamma range fluctuations resulted in an increase of the mean C_{v2} value. The variability of the interspike intervals obtained with Noise 6 was similar to that obtained with PSP 16 ($P = 0.4$), but was higher than the variability obtained with Noise 0 ($P < 0.0001$ between Noise 0 and Noise 6, $P = 0.01$ between PSP 16

and Noise 0). There was also a significant difference between Noise 0 and current pulses ($P < 0.0001$). Figure 8B2,B3 indicates that both reliability and jitter are significantly correlated with the mean C_{v2} value (for reliability: $\rho = 0.675$, $P < 0.0001$; for jitter: $\rho = -0.528$, $P < 0.003$).

Importantly, there was no significant differences in the average firing rate elicited by Noise 0 and Noise 6 ($P = 0.5$) and between PSP 16 and Noise 0 ($P = 0.4$) (not illustrated). However, a significant difference was present between Noise 6 and PSP 16 ($P = 0.05$), yet these two stimuli yielded the closest values in terms of jitter, reliability and variability. That is to say, the differences observed for the three parameters presented in Figure 8 cannot be simply accounted for by differences in firing rate. At present, owing to our small sample size, we are unable to state whether or not there are significant differences in these measures of spike timing between regular spiking cells, fast spiking neurons and intrinsic bursting cells.

In summary, it appears that an increase in the amount of gamma range fluctuation contained in a current waveform leads to an increased probability that action potentials will be fired at a constant *latency* (reliability) and a decreased jitter for the timing of action potentials (precision). At the same time, there is an increased representation of different frequencies in the spike discharge, resulting in an increased variability of *interspike intervals* within each trial, owing to the increased range of frequencies present in the stimulus.

Spike-triggered Averaging of Injected Current

Through spike-triggered averaging of the current injected with the trials Noise 0, Noise 6, and PSP 16 in regular spiking cells, we sought to examine the average components of the injected

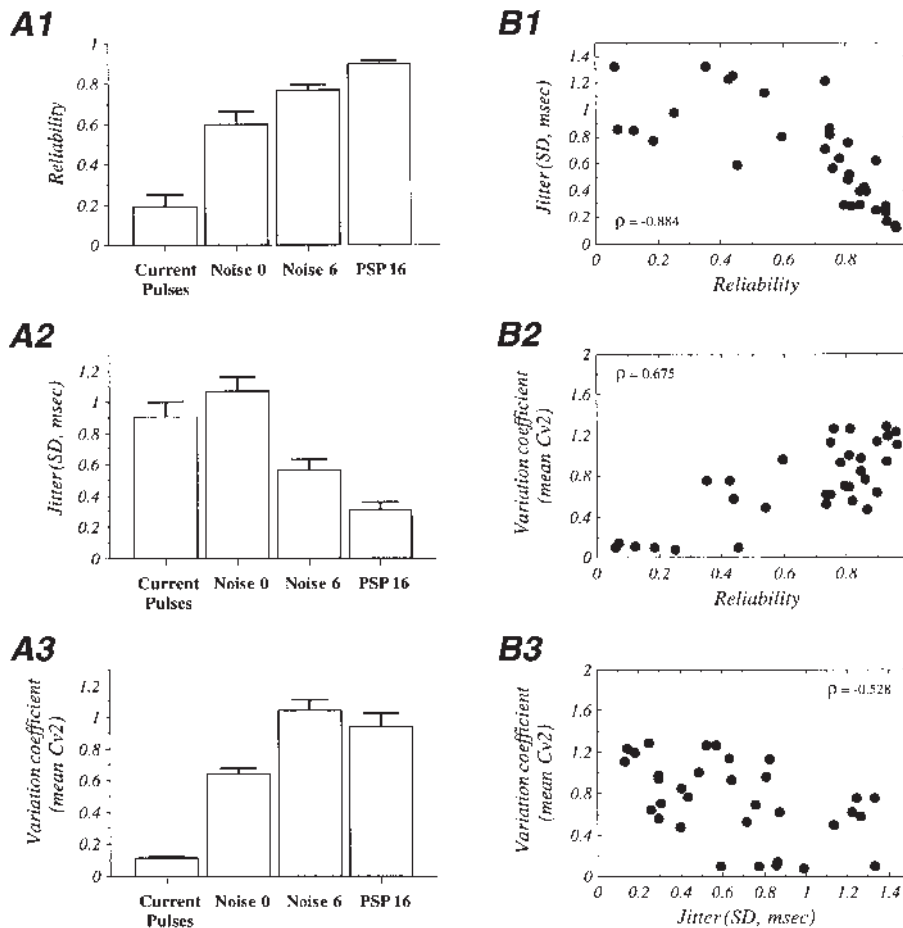


Figure 8. Relationship between stimulation protocol, reliability, jitter and variability. In A1–3 are shown the mean values (error bar = 1 SEM) for *reliability*, *jitter* and interspike interval variation coefficient (C_{v2}), for two artificial current waveforms (Noise 0 and Noise 6) and for a current waveform derived from a visual response (PSP 16). (B1) Scatterplot of *jitter* as a function of *reliability*. (B2) Scatterplot of C_{v2} as a function of *reliability*. (B3) Scatterplot of C_{v2} as a function of *jitter*. In the scatterplot the values obtained with all four stimuli waveforms are pooled together.

Table 1

Summary table for spike latency (*reliability* and *jitter*) and interspike interval variability (C_{v2})

Stimuli	Current pulses ($n = 6$)	Noise 0 ($n = 8$)	Noise 6 ($n = 8$)	PSP 16 ($n = 11$)
<i>Reliability</i>	0.188 ± 0.147	0.596 ± 0.178	0.766 ± 0.076	0.898 ± 0.048
<i>Jitter</i> (ms)	0.897 ± 0.248	1.064 ± 0.246	0.555 ± 0.201	0.307 ± 0.148
Mean C_{v2}	0.108 ± 0.022	0.636 ± 0.095	1.035 ± 0.186	0.931 ± 0.288

Numbers are the mean ± SD. n = number of cell tested with the stimuli.

waveform that are associated with the generation of action potentials (Figure 9). These spike-triggered averages reveal that the generation of action potentials to all three stimuli are associated with depolarizing current injection, as expected. The rate or rise, however, of these injected currents is found to significantly increase, and the duration to decrease, between the protocols Noise 0, Noise 6 and PSP 16, which are associated with increases in spike reliability and decreases in jitter (Figures 8 and 9).

Although it originally contained a large amount of gamma range fluctuation, the spike triggered averaging for PSP 16 current is not oscillatory, while the spike triggered averaging for Noise 6 current displays prominent oscillations. In addition, the autocorrelation histograms computed for the spike discharge elicited by PSP 16 appeared essentially flat, while that computed

from the spike discharge elicited by Noise 6 displayed prominent side peaks (not illustrated). Yet Noise 6 produced a high C_{v2} , almost as high as the one obtained with PSP 16. This result suggests that a signal that is strongly oscillatory can lead to a high variability of interspike intervals. This also indicates that a rhythmic pattern in the synaptic drive is not required to obtain low jitter and high reliability in terms of spike latency, since both parameters were higher with PSP 16 compared to Noise 6.

Precision for Generation of Bursts and Single Spikes in Intrinsic Burst-generating Neurons

Intrinsic burst-generating neurons typically generate a mixture of bursts and single spikes in response to a depolarizing current pulse (Fig. 4C) as well as during the presentation of visual stimuli (L.G. Nowak, R. Azouz, C. Gray and D.A. McCormick, unpublished observations). In response to depolarizing current pulses, these action potential bursts typically occur on the onset of the depolarization and are often followed by a transition to single spike activity (McCormick *et al.*, 1985). Here we examined the reliability and jitter of burst and single spike generation in intrinsically burst-generating neurons in response to injection of a complex waveform, PSP 16 (Figure 10). In the cell illustrated in this figure, bursts consisted of clusters of action potentials with a interspike interval <5 ms. In contrast to constant current pulses, the injection of PSP 16 resulted in the

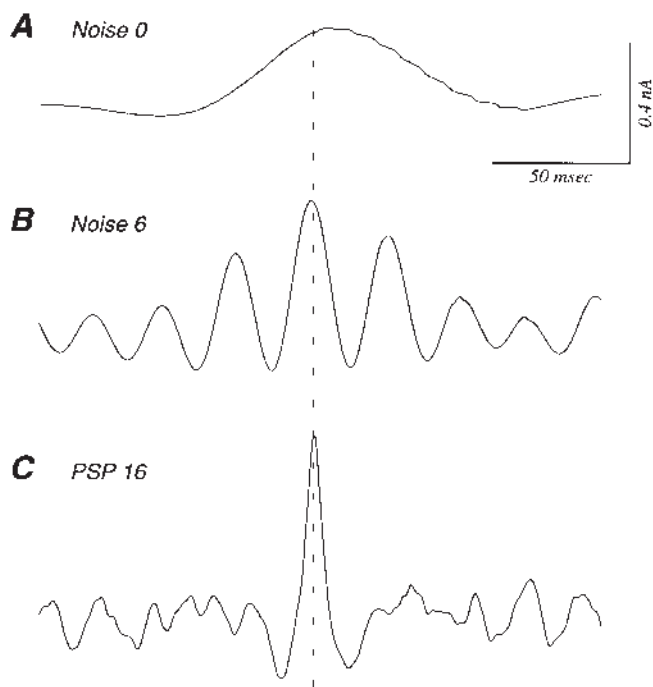


Figure 9. Spike-triggered averaging of injected current. Same cell as in Figures 6 and 7. The vertical dashed line corresponds to the time at which an action potential was triggered by the current injection. (A–C) The spike-triggered average of Noise 0, Noise 6 and PSP 16 current respectively. Note the presence of a prominent oscillatory pattern in the average for Noise 6, but less so in PSP 16, although both current waveform displayed a large amount of power in the gamma range.

generation of both bursts and single spikes throughout the ~ 1 s duration of this stimulus (Fig. 10A–C). In addition, the bursts, represented by larger dots in the raster plots of Figure 10C, consistently occurred at the same latencies with repeated injection of the stimulus. In quantitative terms, the reliability for burst and single spikes were 0.913 and 0.818 respectively, while the jitter was 0.244 for bursts and 0.29 ms for single spikes. Jitter and reliability for bursts and isolated spikes, therefore, were very similar.

Interestingly, spike-triggered averaging of the injected waveform revealed that the components of the injected current associated with the generation of a burst or a single spike were significantly different (Fig. 10D). Single action potentials were preceded by a fast rising current starting directly from the baseline value. In contrast, the current trajectory preceding the first spike of the bursts consisted first in an undershoot below baseline followed by a fast rising depolarizing current. The slope of the rising phase of the current before the isolated spike does not differ from that before the first spike of the burst, although the width of the peak appears slightly larger for bursts compared to single spikes. These results suggest that the undershoot of the current may permit the deinactivation of a conductance that controls burst firing.

Response of Regular Spiking Neurons to Sinewave Currents

The resistive-capacitive properties of cortical neurons predict that they should act as low-pass filters, thereby responding most robustly to low frequency oscillations (Carandini *et al.*, 1996). However, our previous results indicate that higher frequency

activity may have significant effects on the timing of action potential generation. In order to investigate this property more thoroughly, we examined the response of cortical regular spiking neurons to the injection of sinewave currents that continuously varied in frequency from either 2 to 20 or from 10 to 200 Hz and which had both depolarizing and hyperpolarizing components (Figures 11 and 12).

Injection of these waveforms while hyperpolarizing the cell to a negative membrane potential (e.g. -87 mV; Fig. 11A,B) with the intracellular injection of DC demonstrates the low-pass filtering characteristics of cortical neurons. Increasing the frequency of sinewave oscillation from 2 to 200 Hz resulted in a progressively smaller peak-to-peak deviation in the membrane potential.

Application of the same sinewave stimuli when the cell was depolarized by DC injection to near firing threshold (-57 mV; Fig. 11C,D) revealed that the number of action potentials generated per cycle decreased dramatically as the frequency of the stimulus increased, such that at frequencies above ~ 20 Hz, the cell failed to generate action potentials at all (Fig. 11D). However, at frequencies that were successful in causing the regular spiking neuron to discharge, the action potentials are phase-locked with the injection of the sinewave (Fig. 11C,D). This finding suggests that the mid to high frequencies may be capable of strongly influencing spike timing, with a significantly reduced effect on the probability of spike generation.

To test the hypothesis that higher frequency stimuli may strongly modulate spike timing, we examined the response of regular spiking cells to the intracellular injection of Sine20 and Sine200 following depolarization of these neurons via intracellular injection of DC such that they spontaneously discharged at a steady rate of ~ 10 –20 Hz (Fig. 12). Under these conditions, injection of the sinewave stimuli led to increased discharge of the cell at low frequencies (Fig. 12A). However, at frequencies higher than ~ 40 –50 Hz, the sinewave stimulus did not lead to the firing of additional action potentials but instead altered the timing of action potentials such that they phase locked to the stimulus (Fig. 12B–D).

These results suggest that, in natural conditions, low frequencies are responsible for the effective drive of the cells. The higher frequencies within the gamma range may not be powerful enough to trigger additional action potentials, although they are capable of significantly influencing the timing of the action potentials that do occur.

Discussion

Through the intracellular injection of complex waveforms into visual cortical neurons maintained *in vitro* we have demonstrated that regular spiking, fast spiking and burst-generating neurons are all capable of generating action potentials with a high degree of temporal precision and reliability. In addition, we have also confirmed the results of Mainen and Sejnowski (1995) that the high frequency components of the injected waveforms, even if they do not directly elicit action potentials by themselves, are particularly important for determining this temporal precision. We also found that the presence of a broad range of frequencies in the injected waveform insures a broad range of interspike intervals in the resulting action potential discharge, and therefore a high degree of variability in these intervals within single trials. Finally, we demonstrate that gamma range (30–70 Hz) fluctuations in the membrane potential of cortical cells are transmitted to their action potential outputs.

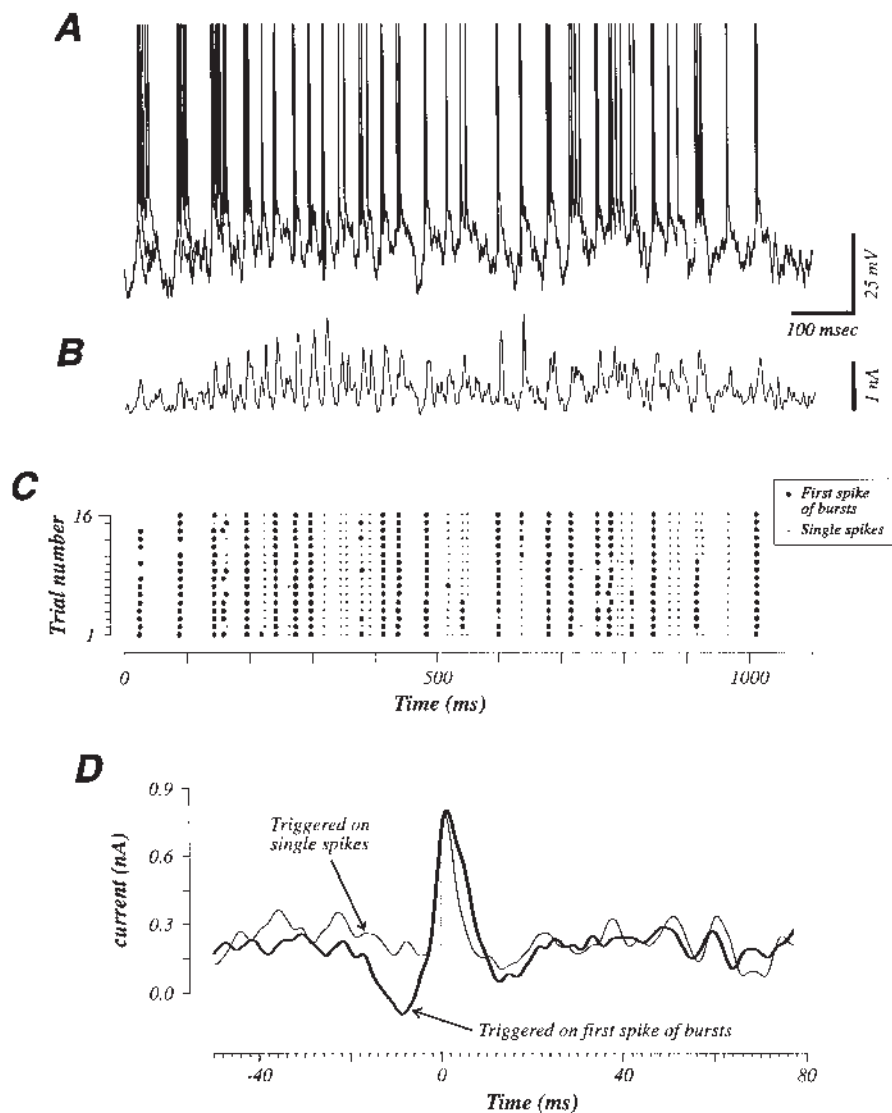


Figure 10. Spike timing reliability and jitter for bursts and single spikes in an intrinsic burst-generating neuron. (A) The cell was an intrinsic burst-generating neuron that discharged either single spikes or bursts of spikes in response to the injection of the stimuli (PSP 16 waveform, shown in B). (C) Raster plot illustrating the precise timing for both single spikes (small dots) and for the first spike of the bursts (large dots). In D are shown averages of the current, triggered either on single spikes (thin line) or on the first spike of the bursts (thick line). The dotted line (time 0) corresponds to action potential generation. Note that, similar to the cell in Figure 9, the spike-triggered averages do not show oscillatory behavior, despite the presence of a large amount of power in the gamma range in the stimulus (Fig. 5). Action potentials are truncated in A.

In vivo recordings of cortical neurons have classically been typified by highly variable responses to constant sensory stimuli. This variability is expressed both in the number of action potentials that are generated as well as the precise time of generation of each action potential from one stimulus to the next (Shiller *et al.*, 1976; Rose, 1979; Dean, 1981; Tolhurst *et al.*, 1983; Bradley *et al.*, 1987; Scobey and Gabor, 1989; Vogels *et al.*, 1989; Snowden *et al.*, 1992; Softky and Koch, 1993; Swindale and Mitchell, 1994). Although a significant portion of this variability results from the activity associated with spontaneous and evoked cortical and thalamocortical rhythms in anesthetized animals (Arieli *et al.*, 1996), or the occurrence of uncontrolled variables such as eye movements in awake behaving animals (Gur *et al.*, 1997), there is also a significant portion that appears to result from the characteristics of cortical and subcortical neuronal circuits and their stimulus-encoding mechanisms (see below).

Two other possible sources for the variability in a single

neuron are an intrinsic randomness in the neuron's spike generating mechanism or an underlying variance in the synaptic inputs. Our study, and that of Mainen and Sejnowski (1995), demonstrate that three major physiological subtypes of cortical cells (regular spiking, fast spiking and burst firing neurons) are all capable of generating action potentials with a high degree of temporal precision when they are stimulated with currents that contain high frequency components resembling barrages of synaptic potentials. This finding indicates that the variability in interspike intervals within trials as well as the variability of the timing and number of action potentials generated with repeated presentation of the same constant stimulus *in vivo* are the result of variations in the underlying synaptic barrages. This variation may result in part from the probabilistic nature of synaptic transmission in cortical networks (see Otmakhov *et al.*, 1993; Stevens and Wang, 1995; Markram, 1997), although this seems unlikely given the high degree of convergence and divergence of synaptic inputs in cortical pathways (e.g. Marsálek *et al.*, 1997).

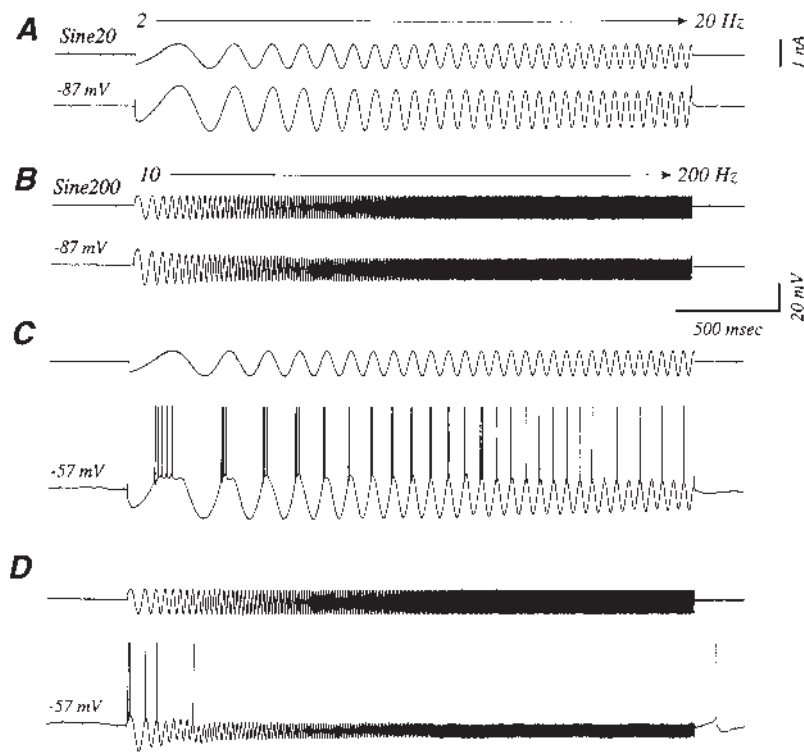


Figure 11. Response of a cell to the injection of a time-varying sinusoidal current (ZAP waveform). Two ZAP waveforms have been used, one for which the frequency varied between 2 and 20 Hz (*A* and *C*), the other for which the frequency varied between 10 and 200 Hz (*B* and *D*). (*A*, *B*) Response during hyperpolarization of the cell to prevent spike generation. The reduction of the amplitude of the membrane potential modulation for high frequencies compared to low ones indicates a stronger filtering for the former. (*C*, *D*) With a small amount of positive DC current injection, the cell fires in response to low frequencies but not to high frequencies, due to their attenuation by the RC characteristics of the cell.

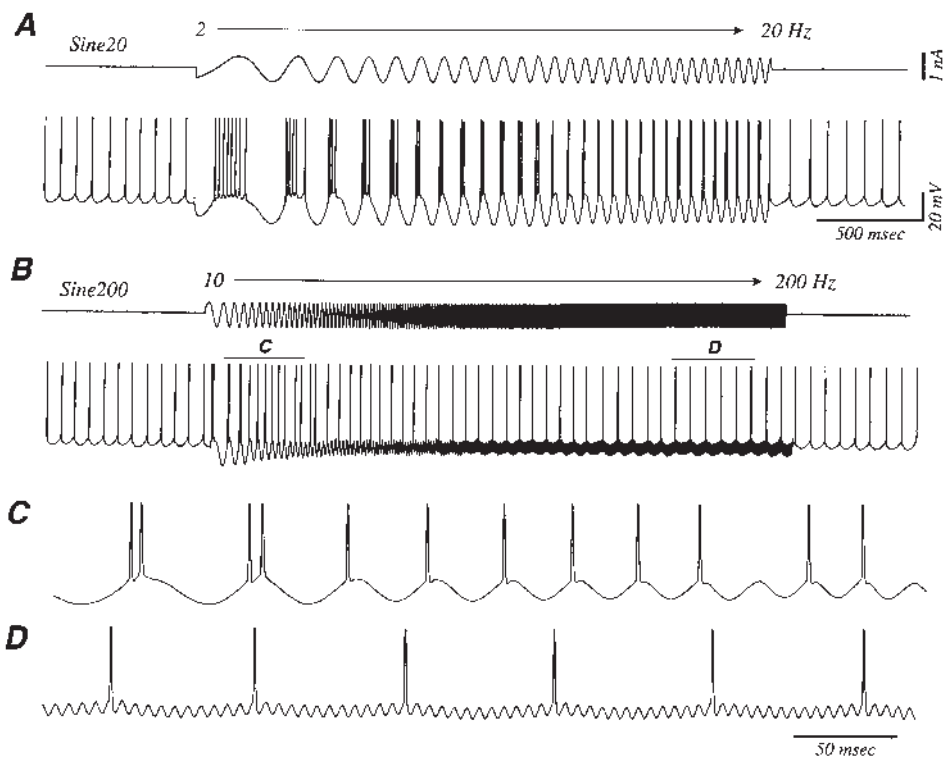


Figure 12. Response of a cell to the injection of a ZAP waveform during spontaneous activity. Same cell as in Figure 11. The cell is depolarized to tonically discharge with the injection of DC prior to injection of the ZAP function. In *A* the injection of the ZAP current in the low frequency range leads to an additional efficient drive of the cell. In *B* the high frequency of the ZAP current does not trigger additional spikes (the cell discharges with the same rate before, during the second half, and after the ZAP current injection). However, action potentials are triggered in phase with the current injected as illustrated in *C* and *D* (higher resolution plot).

Another possibility is that the variation arises (or at least, is maintained) from the balancing of random excitatory and inhibitory synaptic inputs in cortical neurons (e.g. Calvin and Stevens, 1968; Shadlen and Newsome, 1994; van Vreeswijk and Sompolinsky, 1996), or through the synchronization of apparent random EPSPs (Softky and Koch, 1993), and therefore represents a network property.

Subthreshold Mechanisms Involved in Precise Spike Timing

The sources of variation in the generation of each action potential during the injection of constant current pulses or waveforms that contain only low frequencies are not precisely known. During the response to constant current pulses, the precise point of action potential generation is readily influenced by the occurrence of additional sources of current, such as would be expected from the occurrence of spontaneous EPSPs or IPSPs (Reyes and Fetz, 1993a,b). The ability of a depolarizing event to trigger an additional action potential increases as the potassium currents that generate the afterhyperpolarizations following the action potential decrease, and as the membrane potential reaches closer to spike threshold. Therefore, subtle changes in the spontaneous release of excitatory or inhibitory neurotransmitters onto cortical neurons, whether they are dependent or independent of action potential generation in the presynaptic cell, may have significant effects on the timing of action potential generation under these circumstances.

In addition, cortical pyramidal cells also exhibit significant sources of subthreshold noise that is composed of, in part, the stochastic fluctuation in opening and closing of the myriad of different ionic channels present in these neurons (e.g. see DeFelice, 1981). Presumably, this subthreshold activity may also significantly influence the timing of action potential generation when the cell is responding to a constant current pulse or low frequency inputs.

The propensity with which the timing of an action potential is influenced by such extrinsic or intrinsic events is directly proportional to the amount of time that the neuron spends in approaching action potential threshold. Thus, for the response to the injection of a constant current pulse, and in a neuron receiving relatively low frequency activity, the membrane potential may spend a significant period of time repolarizing towards action potential threshold following the generation of the previous action potential. This 'window of opportunity' may then allow for the influence of stochastic fluctuations in ionic currents as well as spontaneous synaptic potentials to advance or retard the precise moment of action potential generation, thus leading to 'jitter'. In contrast, the depolarization of neurons with currents that consist of higher frequencies results in deviations in the membrane potential that may exceed action potential threshold for only relatively brief periods of time. Action potentials can only be generated during these brief periods and therefore this is the only time when small fluctuations in the stochastic properties of ionic currents or synaptic potentials may influence the timing of action potential generation. Since the duration of the depolarization of the membrane potential by high frequency currents is relatively short, the subsequent 'jitter' in action potential timing is also limited (on either side of this depolarization, the membrane potential would rapidly repolarize, decreasing the influence of other inputs), resulting in an increase in the precision with which action potentials are generated. An additional modulating influence is provided by rapid fluctuations in membrane potential associated with higher

frequency activity. The occurrence of a hyperpolarization following the generation of an action potential may facilitate the generation of additional action potentials in response to subsequent depolarizing components by removing inactivation of inward currents associated with action potential generation (e.g. Na^+ or Ca^{2+} currents).

Interestingly the decreased reliability and precision of single neurons to constant current pulses versus 'noisy' stimuli is similar to recent findings in the fly visual system where the presentation of constant-velocity stimuli resulted in a high degree of imprecision in the spike trains of a velocity-sensitive neuron, while presentation of more naturalistic stimuli that contained a mixture of velocities resulted in a very low degree of spike jitter and a high degree of reliability. In this way, the motion-sensitive neuron exhibited a precise temporal relationship between the generation of action potentials and features of the sensory stimulus (de Ruter van Steveninck *et al.*, 1997). These results suggest that neurons embedded in neural networks may be capable of generating precise spike timing when they are activated by the appropriate stimulus.

Studies in the mammalian visual system have also demonstrated the occasional occurrence of precise spike timing and temporal coding. In the retina, maintained *in vitro*, presentation of randomly flickering 'checkerboard' or whole-field stimuli results in action potential discharges that display a high degree of temporal precision and reliability with repeated presentations of the same stimulus, even though there is a low density of spike discharge (Berry *et al.*, 1997). A recent analysis of single unit data from the response of neurons in area MT of the primate cortex, which contains a high density of motion-sensitive neurons, to randomly moving dots has revealed that most cortical neurons respond with a high degree of precision (jitter can be <10 ms) to repeated presentation of the same stimulus if the level of coherence of the motion in the stimulus is low (Bair and Koch, 1996). This result demonstrates that cortical neurons are capable of generating repeated patterns of action potentials in response to a visual stimulus with a high degree of precision and reliability. This high precision is particularly robust in the onset of visual responses, with the rise times remaining equally sharp at different stages of visual processing, from striate to extrastriate (e.g. Marsálek *et al.*, 1997). This low degree of jitter may result from the high incidence of convergence in synaptic inputs in cortical pathways.

Ultimately, the importance of spike timing in individual neurons will only be understood when it is related to the activity of the network of neurons to which the cell is contributing and the influence or role of the cell under question at that time. Indeed, investigations in many neuronal systems, including more recently in the mammalian visual system, have suggested that the relative timing of action potentials between various cells in the network is a key variable in the processing of a sensory stimulus (reviewed in Bialek and Rieke, 1992; Hopfield, 1995; Wehr and Laurent, 1996; Rieke *et al.*, 1997).

Transmission of Gamma Range Fluctuations

Recent experiments demonstrate that synchronized oscillations in the gamma frequency range (30–70 Hz) can occur in the mammalian visual system in a subpopulation of neurons (reviewed in Singer and Gray, 1995; Engel *et al.*, 1997), although their role, if any, in visual processing is still unknown. The resistive and capacitive characteristics of cortical neurons lead to an appreciable filtering of the high frequency content of an input (Carandini *et al.*, 1996; Hutcheon *et al.*, 1996; Figure 11).

Despite this, gamma range fluctuations appear to be transmitted from the input to the spike train: the temporal pattern present in the input is replicated to a significant degree in the action potential output (Figure 5). Carandini *et al.* (1996) recently showed that the high frequencies present in a stimulus waveform can be transmitted to spike activity, provided the stimulus waveform also contained low frequencies. Similarly, we found that the high frequencies present in the ZAP current influenced the spiking activity, provided the ZAP current injection was combined with a DC current injection large enough to drive the cell.

However, the transmission of gamma range fluctuations appears as a noisy process (Figure 5). It could be that this noisiness leads to an attenuation of gamma range fluctuations in the successive steps of processing. This could be avoided if some cells were able to regenerate the gamma range fluctuations. Such 'boosters' could be the chattering cells recently described (Gray and McCormick, 1996). Chattering cells appear to have a propensity to discharge in bursts of action potential in a range restricted, in the highest frequencies, to the upper gamma band (~70 Hz).

Gamma Range Fluctuation and Precise Spike Timing

As a prerequisite to the hypothesis that precise spike timing carries information (if it does), it must be shown that mechanisms exist to sustain it. Gamma range fluctuations could be one of these mechanisms. Better than a low frequency modulation, gamma range fluctuations, since they consist of higher frequency components, lead to precise spike timing. Action potentials may be separated by up to 100 ms, yet they are reproduced at the same latency with a temporal jitter of a fraction of msec (Fig. 6). Low frequency modulation of the membrane potential gives responses that were less reliable, although the temporal jitter would still remain quite small (of the order of 1 ms). Similarly, Mainen and Sejnowski (1995) showed that the precision of spike timing is better for high frequency than low frequency noise.

In addition, the results based on ZAP current injection indicate that gamma range fluctuations, even if they do not efficiently drive the cells, are able to modulate the timing in a very precise way. In that respect our results confirm those obtained by Carandini *et al.* (1996): the low frequencies contained in the stimulus induced synaptic barrage might be viewed as what effectively drives the cells, while the high frequency fluctuations are important in providing precise action potential timing.

Gamma Range Fluctuation and Synchronization on a Short Time Scale

It has been suggested that synchronization on a short time scale might provide a means to unify the distributed neuronal activities induced by the multiple features of an object into one coherent percept (the binding by synchronization hypothesis; for review see Milner, 1974; Damasio, 1990; Engel *et al.*, 1992; Aertsen and Arndt, 1993; Gray, 1994; Engel *et al.*, 1997; see, however, Fahle and Koch, 1995; Kiper *et al.*, 1996). Precisely synchronized activity manifests itself by narrow peaks (with widths down to a few milliseconds) in cross-correlation histograms. As far as visual cortex is concerned, such narrow peaks have been reported in a number of studies, in both cat and monkey, and for both intra- and interareal interactions (reviewed in Fetzer *et al.*, 1991; Aertsen and Arndt, 1993; Singer and Gray, 1995; see also Das and Gilbert, 1995; Nowak *et al.*, 1995; Sillito

et al., 1995; Kreiter and Singer, 1996; Livingstone, 1996). These narrow peaks also correspond to the central structure visible in oscillatory cross correlation histograms (see Gray and Singer, 1995).

It has been proposed that gamma frequency ('40 Hz') oscillations play a role in promoting precise synchronization of neuronal activity (Engel *et al.*, 1992; Gray, 1994; however, see Koch and Schuster, 1992). Our results suggest that this should be extended to higher frequency fluctuations that do not show an oscillatory pattern. The presence of a narrow peak in a cross-correlation histogram requires that the two recorded neurons be activated at the same time by 'common' EPSPs. It also requires that action potential timing be extremely precise in the two recorded cells, with respect to the depolarizing events that trigger them. As shown in Figures 6 and 8, such precision is better achieved with higher rather than lower frequency modulations. However, the high temporal precision does not require an oscillatory structure in the input (Figure 9). In parallel with that observation, it has been shown that changing the features of a visual stimulus can transform an oscillatory cross-correlation histogram into one that contains just a central peak, without satellite peaks (Schwartz and Bolz, 1991; Nowak *et al.*, 1995), indicating that the rhythmicity might be lost without loss of synchrony. In other words, precise synchronization may be sustained by high frequency (gamma range) fluctuations, even in the lack of clear rhythmicity in the signal.

The results we have presented illustrate the ability of multiple types of cortical neurons to generate highly precise temporal patterns of action potentials (see also Mainen and Sejnowski, 1995). Through the use of the temporal domain, neurons may more efficiently transmit information concerning the stimulus than if they utilized a rate code alone (see Rieke *et al.*, 1997), although the nature of these temporal codes, if they exist, remains to be revealed. Hopefully, the combination of *in vivo*, *in vitro* and *in computo* experiments will help to clarify this issue and provide new insights on the functioning of cortical networks.

Notes

We thank Terry Sejnowski and Charles Gray for their comments on the manuscript. This work was supported by the National Institute of Health and the Fyssen Foundation.

Address correspondence to D.A. McCormick, Section of Neurobiology, Yale University School of Medicine, 333 Cedar Street, New Haven, CT 06510, USA.

References

- Abeles M, Gerstein GL (1988) Detecting spatiotemporal firing patterns among simultaneously recorded single neurons. *J Neurophysiol* 60:909-924.
- Abeles M, Bergman H, Margalit E, Vaadia E (1993) Spatiotemporal firing patterns in the frontal cortex of behaving monkeys. *J Neurophysiol* 70:1629-1638.
- Aertsen A, Arndt M (1993) Response synchronization in the visual cortex. *Curr Opin Neurobiol* 3:586-594.
- Arieli A, Sterkin A, Grinvald A, Aertsen A (1996) Dynamics of ongoing activity: explanation of the large variability in evoked cortical responses. *Science* 273:1868-1871.
- Bair W, Koch C (1996) Temporal precision of spike trains in extrastriate cortex of the behaving macaque monkey. *Neural Comp* 8:1185-1202.
- Bradley A, Skottun BC, Ohzawa I, Sclar G, Freeman RD (1987) Visual orientation and spatial frequency discrimination: a comparison of single neurons and behavior. *J Neurophysiol* 57:755-772.
- Berry MJ, Warland DK, Meister M (1997) The structure and precision of retinal spike trains. *Proc Natl Acad Sci USA* (in press).
- Bialek W, Rieke F (1992) Reliability and information transmission in spiking neurons. *Trends Neurosci* 15:428-434.

- Calvin WH, Stevens CF (1968) Synaptic noise and other sources of randomness in motoneuron interspike intervals. *J Neurophysiol* 31: 574-587.
- Carandini M, Mechler F, Leonard CS, Movshon JA (1996) Spike train encoding by regular-spiking cells of the visual cortex. *J Neurophysiol* 76:3425-3441.
- Croner LJ, Purpura K, Kaplan E (1993) Response variability in retinal ganglion cells of primates. *Proc Natl Acad Sci USA* 90: 8128-8130.
- Damasio AR (1990) Synchronous activation in multiple cortical regions: A mechanism for recall. *Semin Neurosci* 2:287-296.
- Das A, Gilbert CD (1995) Receptive field expansion in adult visual cortex is linked to dynamic changes in strength of cortical connections. *J Neurophysiol* 74:779-792.
- Dayoff JE, Gerstein GL (1983) Favored patterns in spike trains. II. Application. *J Neurophysiol* 49:1349-1363.
- de Ruyter van Steveninck RR, Lewen GD, Strong SP, Koberle R, Bialek W (1997) Reproducibility and variability in neural spike trains. *Science* 275:1805-1808.
- Dean AF (1981) The variability of discharge of simple cells in the cat striate cortex. *Exp Brain Res* 44:437-440.
- DeFelix LJ (1981) Introduction to membrane noise. New York: Plenum Press.
- Engel AK, König P, Singer W (1991) Direct physiological evidence for scene segmentation by temporal coding. *Proc Natl Acad Sci USA* 88:9136-9140.
- Engel AK, König P, Kreiter AK, Schillen TB, Singer W (1992) Temporal coding in the visual cortex: new vistas on integration in the nervous system. *Trends Neurosci* 15:218-226.
- Engel AK, Roelfsema PR, Fries P, Brecht M, Singer W (1997) Role of temporal domain for response selection and perceptual binding. *Cereb Cortex* 7:571-582.
- Fahle M, Koch C (1995) Spatial displacement, but not temporal asynchrony, destroy figural binding. *Vision Res* 35:491-494.
- Fetz EE, Toyama K, Smith W (1991) Synaptic interactions between cortical neurons. In *Cerebral cortex*, vol. 9 (Peters A, ed.), pp 1-47. New York: Plenum Press.
- Gray CM (1994) Synchronous oscillations in neuronal systems: mechanisms and functions. *J Comp Neurosci* 1:11-38.
- Gray CM, McCormick DA (1996) Chattering cells: superficial pyramidal neurons contributing to the generation of synchronous oscillations in the visual cortex. *Science* 274:109-113.
- Gray CM, König P, Engel AK, Singer W (1989) Oscillatory responses in cat visual cortex exhibit inter-columnar synchronization which reflects global stimulus properties. *Nature* 338:334-337.
- Gray CM, Engel AK, König P, Singer W (1990) Stimulus-dependent neuronal oscillations in cat visual cortex: receptive field properties and feature dependence. *Eur J Neurosci* 2:607-619.
- Gur M, Beylin A, Snodderly DM (1997) Response variability of neurons in primary visual cortex (V1) of alert monkeys. *J Neurosci* 17:2914-2920.
- Hartveit E, Heggelund P (1994) Response variability of single cells in the dorsal lateral geniculate nucleus of the cat. Comparison with retinal input and effect of brainstem stimulation. *J Neurophysiol* 72: 1278-1289.
- Holt FGR, Softky WR, Koch C, Douglas RJ (1996) Comparison of discharge variability *in vitro* and *in vivo* in cat visual cortex neurons. *J Neurophysiol* 75:1806-1814.
- Hopfield JJ (1995) Pattern recognition computation using action potential timing for stimulus representation. *Nature* 376:33-36.
- Hutcheon B, Miura RM, Puij E (1996) Subthreshold membrane resonance in neocortical neurons. *J Neurophysiol* 76:683-697.
- Jagadeesh B, Gray CM, Ferster D (1992) Visually evoked oscillations of membrane potential in cells of at visual cortex. *Science* 257:552-554.
- Kiper DC, Gegenfurtner KR, Movshon JA (1996) Cortical oscillatory responses do not affect visual segmentation. *Vis Res* 36:539-544.
- Koch C, Schuster H (1992) A simple network showing burst synchronization without frequency locking. *Neural Comput* 4:211-223.
- Kreiter AK, Singer W (1996) Stimulus-dependent synchronization of neuronal responses in the visual cortex of the awake macaque monkey. *J Neurosci* 16:2381-2396.
- Lestienne R, Strehler BL (1987) Time structure and stimulus dependence of precisely replicating patterns present in monkey cortical neuronal spike trains. *Brain Res* 437:214-238.
- Livingstone MS (1996) Oscillatory firing and interneuronal correlations in squirrel monkey striate cortex. *J Neurophysiol* 75:2467-2485.
- Mainen ZF, Sejnowski TJ (1995) Reliability of spike timing in neocortical neurons. *Science* 268:1503-1506.
- Markram H (1997) A network of thick tufted layer 5 pyramidal neurons. *Cereb Cortex* 7:523-533.
- Marsálek P, Koch C, Maunsell J (1997) On the relationship between synaptic input and spike output jitter in individual neurons. *Proc Natl Acad Sci USA* 94:735-740.
- McCormick DA, Connors BW, Lighthall JW, Prince DA (1985) Comparative electrophysiology of pyramidal and sparsely spiny neurons of the neocortex. *J Neurophysiol* 54:782-806.
- Milner PM (1974) A model for visual shape recognition. *Physiol Rev* 81:521-535.
- Nowak LG, Munk MHJ, James AC, Nelson JI, Bullier J (1995) The structural basis of cortical synchronization. I. 3 types of inter-hemispheric coupling. *J Neurophysiol* 74:2379-2400.
- Otmakhov N, Shirke AM, Malinow R (1993) Measuring the impact of probabilistic transmission on neuronal output. *Neuron* 10: 1101-1111.
- Reyes AD, Fetz EE (1993a) Two modes of interspike interval shortening by brief transient depolarizations in cat neocortical neurons. *J Neurophysiol* 69:1661-1672.
- Reyes AD, Fetz EE (1993b) Effects of transient depolarizing potentials on the firing rate of cat neocortical neurons. *J Neurophysiol* 69:1673-1683.
- Rieke F, Warland D, de Ruyter van Steveninck R, Bialek W (1997) Spikes. Exploring the neural code. Cambridge, MA: MIT Press.
- Rose D (1979) An analysis of the variability of unit activity in the cat's visual cortex. *Exp Brain Res* 37:565-604.
- Schiller PH, Finlay BL, Volman SF (1976) Short-term response variability of monkey striate neurons. *Brain Res* 105:347-349.
- Schwarz C, Bolz J (1991) Functional specificity of a long-range horizontal connection in cat visual cortex: a cross-correlation study. *J Neurosci* 11:2995-3007.
- Scobey RP, Gabor AJ (1989) Orientation discrimination sensitivity of single units in cat primary visual cortex. *Exp Brain Res* 77:398-406.
- Shadlen MN, Newsome WT (1994) Noise, neural codes and cortical organization. *Curr Opin Neurobiol* 4:569-579.
- Sillito AM, Grieve KL, Jones HE, Cudeiro J, Davies J (1995) Visual cortical mechanisms detecting focal orientation discontinuities. *Nature* 378:492-496.
- Singer W, Gray CM (1995) Visual feature integration and the temporal correlation hypothesis. *Annu Rev Neurosci* 18:555-586.
- Snoden RJ, Treue S, Anderson RA (1992) The response of neurons in areas V1 and MT of the alert rhesus monkey to moving random dot patterns. *Exp Brain Res* 88:389-400.
- Softky W (1995) Simple codes versus efficient codes. *Curr Opin Neurobiol* 5: 239-247.
- Softky W, Koch C (1993) The highly irregular firing of cortical cells is inconsistent with temporal integration of random EPSPs. *J Neurosci* 13:334-350.
- Stevens CF, Wang Y (1995) Facilitation and depression at single central synapses. *Neuron* 14: 795-802.
- Swindale NV, Mitchell DE (1994) Comparison of receptive field properties of neurons in area 17 of normal and bilaterally amblyoptic cats. *Exp Brain Res* 99:399-410.
- Tang AC, Bartels AM, Sejnowski TJ (1997) Effects of cholinergic modulation on responses of neocortical neurons to fluctuating input. *Cereb Cortex* 7:502-509.
- Tollhurst DJ, Movshon JA, Dean AF (1983) The statistical reliability of signals in single neurons in cat and monkey visual cortex. *Vis Res* 23: 775-785.
- Troy JB, Lennie P (1987) Detection latencies of X and Y type cells of the cat's dorsal lateral geniculate nucleus. *Exp Brain Res* 65:703-706.
- van Vreeswijk C, Sompolinsky H (1996) Chaos in neuronal networks with balanced excitatory and inhibitory activity. *Science* 274:1724-1726.
- Villa AE, Fuster JM (1992) Temporal correlates of information processing during visual short-term memory. *Neuroreport* 3:113-116.
- Villa AE, Abeles M (1990) Evidence for spatiotemporal firing patterns within the auditory thalamus of the cat. *Brain Res* 509:325-327.
- Vogels R, Spileers W, Orban GA (1989) The response variability of striate cortical neurons in the behaving monkey. *Exp Brain Res* 77:432-436.
- Wehr M, Laurent G (1996) Odour encoding by temporal sequences of firing in oscillating neural assemblies. *Nature* 384:162-166.